JEM Journal of Experimental Medicine

ARTICLE

Hes1 attenuates type I IFN responses via VEGF-C and WDFY1

Fei Ning[1,2,3], Xiaoyu Li[1,3], Li Yu[1,2,3], Bin Zhang[1,3], Yuna Zhao[4], Yu Liu[5], Baohong Zhao[6,7], Yingli Shang[4], and Xiaoyu Hu[1,3]

Induction of type I interferons (IFNs) is critical for eliciting competent immune responses, especially antiviral immunity. However, uncontrolled IFN production contributes to pathogenesis of autoimmune and inflammatory diseases. We found that transcription factor Hes1 suppressed production of type I IFNs and expression of IFN-stimulated genes. Functionally, Hes1-deficient mice displayed a heightened IFN signature in vivo, mounted enhanced resistance against encephalomyocarditis virus infection, and showed signs of exacerbated experimental lupus nephritis. Mechanistically, Hes1 did not suppress IFNs via direct transcriptional repression of IFN-encoding genes. Instead, Hes1 attenuated activation of TLR upstream signaling by inhibition of an adaptor molecule, WDFY1. Genome-wide assessment of Hes1 occupancy revealed that suppression of WDFY1 was secondary to direct binding and thus enhancement of expression of VEGF-C by Hes1, making *Vegfc* a rare example of an Hes1 positively regulated gene. In summary, these results identified Hes1 as a homeostatic negative regulator of type I IFNs for the maintenance of immune balance in the context of antiviral immunity and autoimmune diseases.

Introduction

Induction of type I IFNs, such as IFN-α and IFN-β, is a critical event for host defense during viral and bacterial infections (McNab et al., 2015; Boxx and Cheng, 2016). IFN-α and IFN-β further activate downstream signaling pathways that lead to transcriptional induction of a wide range of IFN-stimulated genes (ISGs) encoding key immune effector molecules, including but not limited to translation inhibitors, chemokines, and antigen-presenting molecules (Ivashkiv and Donlin, 2014; Schneider et al., 2014; Wong and Chen, 2016). However, excessive IFN production often acts as an amplifier of undesirable autoimmune and inflammatory responses and has been causally linked to pathogenesis of autoimmune diseases such as systemic lupus erythematosus (SLE; Hall and Rosen, 2010; Rönnblom et al., 2011; Crow, 2014). Pharmacologically dampening either IFN expression or IFN signaling has shown clear beneficial effects in animal models of lupus (Nacionales et al., 2007; Urbonaviciute et al., 2013). More importantly, anti-IFN therapies are being actively investigated in clinical trials for treatment of SLE (Petri et al., 2013; Kalunian et al., 2016; Khamashta et al., 2016; Furie et al., 2017). To rationally design pharmacological interventions targeting IFNs in human diseases, comprehensive understanding of positive and negative regulatory mechanisms controlling the magnitude and duration of IFN production is much desired. Type I IFNs are typically upregulated by the activation of a cascade of signaling molecules downstream of pattern recognition receptors, converging at transcriptional induction of IFN genes by IFN regulatory factor (IRF) family transcription factors. This multistep process starting from receptor signaling to transcription activation provides ample opportunities for negative regulatory factors to exert their inhibitory actions (Kondo et al., 2012; Chen et al., 2017). For example, noncanonical NF-κB has been shown to suppress signal-induced histone modification at the *Ifnb1* locus by viruses and TLR ligands (Jin et al., 2014). However, due to the necessity of tightly controlling IFN production and the complex nature of intermolecular interactions, our understanding of the mechanisms governing negative regulation of IFNs is incomplete and requires further investigation and clarification.

Transcription factor hairy and enhancer of split 1 (Hes1) belongs to a family of basic helix-loop-helix DNA-binding proteins best known for their identities as Notch targets (Kobayashi and Kageyama, 2014). Given the critical role of Notch in cell fate decisions, functions of Hes family members have been studied predominantly in the context of developmental biology. Ablation

[1]Institute for Immunology and School of Medicine, Tsinghua University, Beijing, China; [2]Tsinghua-Peking Center for Life Sciences, Tsinghua University, Beijing, China; [3]Beijing Key Laboratory for Immunological Research on Chronic Diseases, Beijing, China; [4]Shandong Provincial Key Laboratory of Animal Biotechnology and Disease Control & Prevention, College of Veterinary Medicine, Shandong Agricultural University, Taian, China; [5]State Key Laboratory of Virology, Medical Research Institute, College of Life Sciences, Wuhan University, Wuhan, China; [6]Arthritis and Tissue Degeneration Program, David Z. Rosensweig Genomics Research Center, Hospital for Special Surgery, New York, NY; [7]Department of Medicine, Weill Cornell Medical College, New York, NY.

Correspondence to Xiaoyu Hu: xiaoyuhu@tsinghua.edu.cn; Yingli Shang: shangyl@sdau.edu.cn.

of Hes1 in mice leads to embryonic or neonatal lethality due to premature neuronal differentiation and severe neural tube defects (Ishibashi et al., 1995). To date, knowledge about Hes family proteins in the immune system remains scarce. We have previously reported that Hes1 inhibits TLR-mediated induction of cytokines and chemokines such as IL-6, IL-12, and CXCL1 in macrophages (Hu et al., 2008; Shang et al., 2016a), identifying Hes1 as a negative regulator of innate immune responses. More recently, we found that epithelial Hes1 deficiency leads to intestinal microbial dysbiosis and disturbed homeostasis (Guo et al., 2018). In addition to its emerging role in immune regulation, an accumulating body of literature has implicated Notch target genes in the regulation of autoimmune disorders such as SLE (Shang et al., 2016b). For example, Hes1 expression was found to be lower in patients with active SLE than in healthy controls (Sodsai et al., 2008), raising the interesting possibility that dysregulation of Notch target genes such as Hes1 may contribute to SLE pathogenesis. Given that SLE is an autoimmune disease prominently featured with a heightened IFN signature, it would be of importance to investigate functional as well as molecular connections between Hes1 and IFNs, which remain uncharacterized.

WD-repeat and FYVE-domain–containing protein 1 (WDFY1) colocalizes with early endosome via the FYVE domain and acts as an adaptor molecule for protein–protein interactions (Ridley et al., 2001). Limited functional studies of WDFY1 indicated that *Wdfy1* expression was associated with aging (Arisi et al., 2011; Bennett et al., 2015), but the exact physiological function and regulation of WDFY1 remain obscure. Recent reports have identified WDFY1 as a new adaptor protein for TLR3/4 signaling by interacting with TLR3/4 and facilitating recruitment of Toll/IL-1 receptor domain–containing adaptor-inducing IFN-β (TRIF) to these receptors (Hu et al., 2015; Nandakumar and Paludan, 2015), suggesting a role of WDFY1 in innate immune responses. As for regulation of WDFY1 expression, two studies reported that WDFY1 transcription is negatively regulated by a cell surface receptor neuropilin-2 (NRP2) in cancer cells (Stanton et al., 2013; Dutta et al., 2016). Interestingly, NRP2 also mediates signaling by vascular endothelial growth factor C (VEGF-C; Yao and Bouyain, 2015; Schellenburg et al., 2017), although it is not clear whether VEGF-C can regulate expression of WDFY1 in immune cells.

In this study, we explored the role of Hes1 in regulating expression of key immune effector molecules, type I IFNs. We demonstrated that Hes1 negatively regulated expression of type I IFNs and ISGs at both basal and TLR-stimulated conditions. As a result of heightened IFN expression, Hes1-deficient mice displayed an enhanced IFN signature, increased resistance against encephalomyocarditis virus (EMCV) infection, and exacerbated experimental lupus nephritis in vivo. Mechanistically, Hes1-mediated suppression of type I IFNs was through regulating the expression of a newly identified TLR signaling adaptor protein, WDFY1, via modulating its upstream inhibitory factor, VEGF-C. The molecular connections between Hes1 and VEGF-C–WDFY1 were functionally validated in vivo in viral infection and experimental lupus models. Thus, our findings identify Hes1 as a crucial homeostatic suppressor of type I IFNs via targeting the VEGF-C–WDFY1 axis and deepen our understanding of mechanisms curbing IFN responses under physiological and pathological conditions.

Results

Hes1 deficiency promotes the expression of type I IFNs and ISGs in macrophages

To explore the potential connections between Hes1 and type I IFNs, we generated $Hes1^{fl/fl}Cre\text{-}ER^{T2}$ mice in which deletion of the *Hes1* gene was achieved by tamoxifen administration (referred to hereinafter as Hes1 KO; Indra et al., 1999). To induce IFN expression, bone marrow–derived macrophages (BMDMs) from $Hes1^{fl/fl}Cre\text{-}ER^{T2}$ mice that showed efficient deletion of the *Hes1* gene (Fig. S1 A) and $Hes1^{+/+}Cre\text{-}ER^{T2}$ control BMDMs were stimulated with poly(I:C) (polyinosinic:polycytidylic acid), a synthetic mimic of viral double-stranded RNA (dsRNA) that mainly activates TLR3 signaling. RNA sequencing (RNA-seq)–based global gene expression profiling analysis of poly(I:C)-treated BMDMs revealed that 49 genes were overexpressed greater than twofold in Hes1 KO BMDMs relative to their expression levels in control cells. Among them, a subset of the overexpressed genes exhibited heightened baseline transcript levels in unstimulated Hes1 KO cells (Fig. 1 A). Notably, approximately two-thirds of these Hes1-restrained genes were ISGs according to the Interferome database (Rusinova et al., 2013; Fig. 1 B). Enhanced induction of a subset of well-known ISGs, including genes encoding the IFN-induced GTPase superfamily (*Iigp1*), the guanylate-binding protein subfamily (*Gbp4*, *Gbp5*, *Gbp6*, and *Gbp9*), the GTP-binding protein myxoma subfamily (*Mx1* and *Mx2*), chemokines (*Cxcl9*, *Cxcl10*, and *Ccl12*), and IFN-induced protein with tetratricopeptide repeats (*Ifit1*, *Ifit2*, and *Ifit3*), in Hes1-deficient macrophages was further confirmed by quantitative real-time PCR (qPCR; Fig. 1 C). Thus, these results indicated that Hes1 negatively regulated TLR3-mediated induction of ISGs.

Expression of ISGs is generally driven by IFN signaling via activation of transcription factors STAT1 and STAT2, which form a heterotrimeric complex with IRF9 to induce ISG transcription (Ivashkiv and Donlin, 2014). To determine whether Hes1 suppressed ISG expression directly through transcriptional regulation of ISGs or indirectly through modulating events upstream of IFNs, we stimulated Hes1-deficient BMDMs and control cells with IFN-β to directly activate ISG expression and found that IFN-β stimulation induced comparable expression of ISGs, including *Mx1*, *Cxcl9*, and *Ccl12*, in WT and Hes1 KO macrophages (Figs. 1 D and S1 B), indicating that Hes1 may not directly regulate transcription of ISGs. Instead, enhanced phosphorylation of STAT1 and STAT2 was observed in Hes1-deficient BMDMs in response to poly(I:C) stimulation (Fig. 1 E). In addition, blockade of type I IFN signaling using an antibody against IFNAR1 abrogated poly(I:C)-mediated induction of ISGs in both WT and Hes1 KO cells (Fig. S1 C). These data suggested that Hes1 likely impaired molecular events upstream of IFN signaling, such as production of type I IFNs. Indeed, Hes1 deficiency led to enhanced *Ifnb1* mRNA expression, as evidenced by both expression profiling analysis (Fig. 1 A) and qPCR results

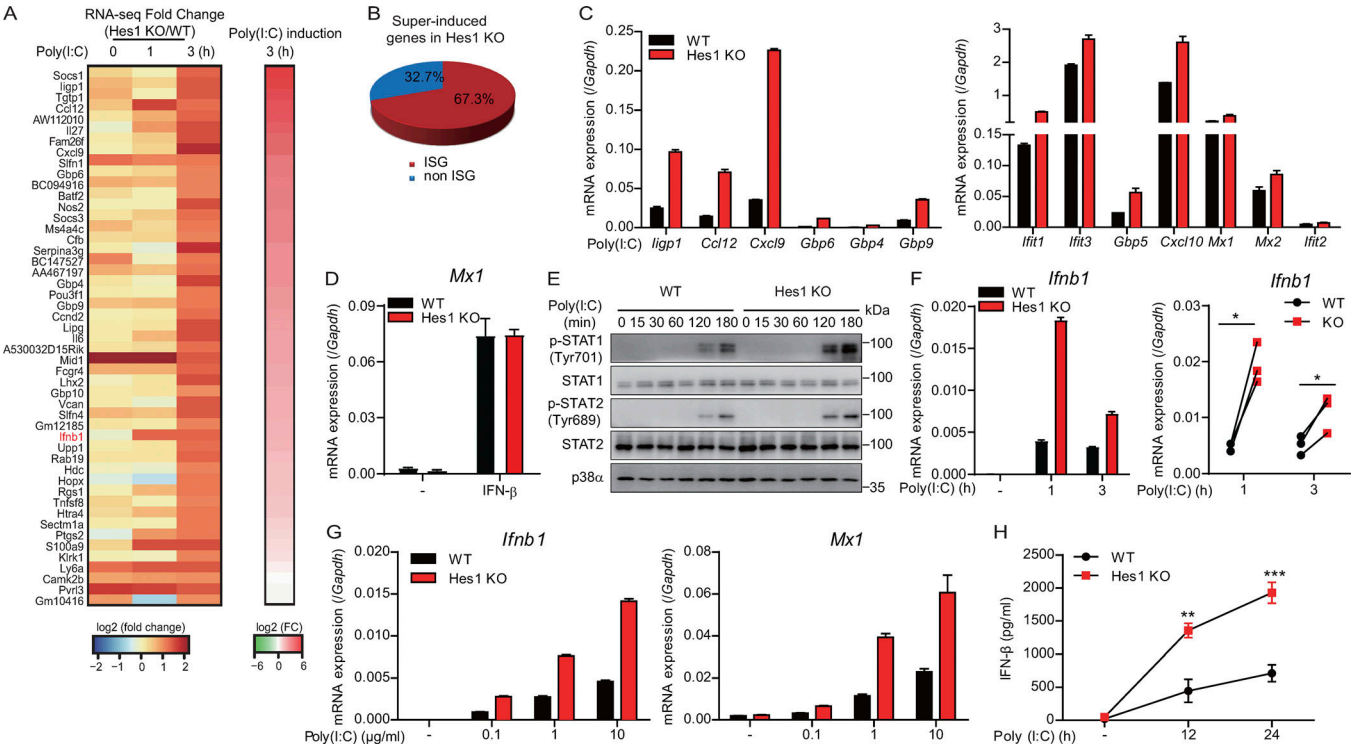

Figure 1. **Hes1 deficiency results in enhanced TLR3-induced expression of type I IFN and ISGs. (A)** Heatmap of superinduced genes by poly(I:C) in *Hes1*$^{fl/fl}$*Cre-ER*^{T2} (Hes1 KO) BMDMs versus *Hes1*$^{+/+}$*Cre-ER*^{T2} (WT) cells. BMDMs were stimulated without or with 1 µg/ml poly(I:C) for the indicated periods. *Ifnb1* in listed genes is highlighted in red. FC, fold change. **(B)** Percentage of ISGs (defined on the Interferome database) among all superinduced genes by poly(I:C) at 3 h in Hes1 KO BMDMs. **(C)** qPCR analysis of ISG mRNA in WT and Hes1 KO BMDMs stimulated with poly(I:C) for 3 h. **(D)** qPCR analysis of *Mx1* in WT and Hes1 KO BMDMs stimulated with IFN-β (10 U/ml) for 3 h. **(E)** Immunoblotting analysis of phosphorylated (p-) and total STAT1 (Tyr701) and STAT2 (Tyr689) in whole-cell lysates of WT and Hes1 KO BMDMs stimulated with poly(I:C) for various times (top lanes). Levels of p38α served as loading controls. **(F)** qPCR analysis of *Ifnb1* in WT and Hes1 KO BMDMs stimulated with poly(I:C) for various times (left). Cumulative results of *Ifnb1* expression are shown (right). **(G)** qPCR analysis of *Ifnb1* and *Mx1* in WT and Hes1 KO BMDMs stimulated with various concentrations of poly(I:C) (horizontal axes) for 2 h. **(H)** ELISA of IFN-β in supernatant of WT and Hes1 KO BMDMs stimulated with poly(I:C) for various times (horizontal axes). Data are representative of one (A and B) or three independent experiments (C–E, F [left], and G; mean + SD of technical triplicates in C, D, F [left], and G) or are pooled from three (F [right] and H; mean ± SD in H) independent experiments. *, P < 0.05; **, P < 0.01; ***, P < 0.001 (Student's *t* test).

in multiple independent experiments (Fig. 1 F). In addition, superinduction of *Ifnb1* and *Mx1* in Hes1-deficient macrophages was observed over a wide range of poly(I:C) doses, suggesting that Hes1-mediated suppression of these genes was a robust effect independent of activator dosages (Fig. 1 G). Consistent with the mRNA results, levels of IFN-β protein were also higher in the supernatants of Hes1-deficient BMDMs than in those of Hes1-sufficient cells (Fig. 1 H). Moreover, increased expression of *Ifnb1* in response to poly(I:C) stimulation was also observed in macrophages derived from mice with myeloid-specific Hes1 deletion using *Lyz2-Cre* (Fig. S1 D), implying that Hes1-mediated regulation of IFNs was a highly reproducible phenomenon independent of the gene deletion methods. As *Cre-ER*^{T2} achieved a more efficient gene deletion than *Lyz2-Cre*, we chose to use the *Hes1*$^{fl/fl}$*Cre-ER*^{T2} system for most of the in vitro experiments in this study. Given that poly(I:C) activates TLR3 that shares IFN-inducing signaling modules with TLR4, we assessed whether Hes1-associated hyperinduction of IFNs was also observed upon stimulation with a TLR4 ligand, LPS. Indeed, LPS stimulation also led to superinduction of *Ifnb1* and *Mx1* in Hes1-deficient macrophages (Fig. S1 E). Taken together, the above multiple lines of genetic loss-of-function evidence supported that Hes1 functions as a homeostatic suppressor of type I IFNs and ISGs.

Hes1 deficiency promotes antiviral immunity

Type I IFNs are key mediators of host antiviral immune responses. Given that poly(I:C) is a synthetic analogue of viral dsRNA, we investigated the role of Hes1 in host responses to EMCV infection, which involved TLR3-mediated recognition of viral dsRNA (Hardarson et al., 2007). Upon EMCV infection of primary macrophages, Hes1 deficiency led to enhanced induction of *Ifnb1*, *Ifna4*, and ISGs (*Cxcl10*, *Mx1*, and *Mx2*; Fig. 2, A and B). Concomitantly, virus titers were lower in Hes1-deficient BMDMs than in WT cells, as measured by expression of the EMCV RNA (Fig. 2 C). To further elucidate the physiological role of Hes1 in host antiviral immune responses in vivo, we generated animals deficient of Hes1 in the hematopoietic compartment by transferring bone marrow cells from Hes1$^{+/+}$*Cre-ER*^{T2} or *Hes1*$^{fl/fl}$*Cre-ER*^{T2} mice into irradiated C57BL/6J recipients (Fig. 2 D) and subsequently challenged these chimeric mice with EMCV. In response to a sublethal dose of EMCV infection, levels of IFN-β in the serum of Hes1-deficient mice were significantly

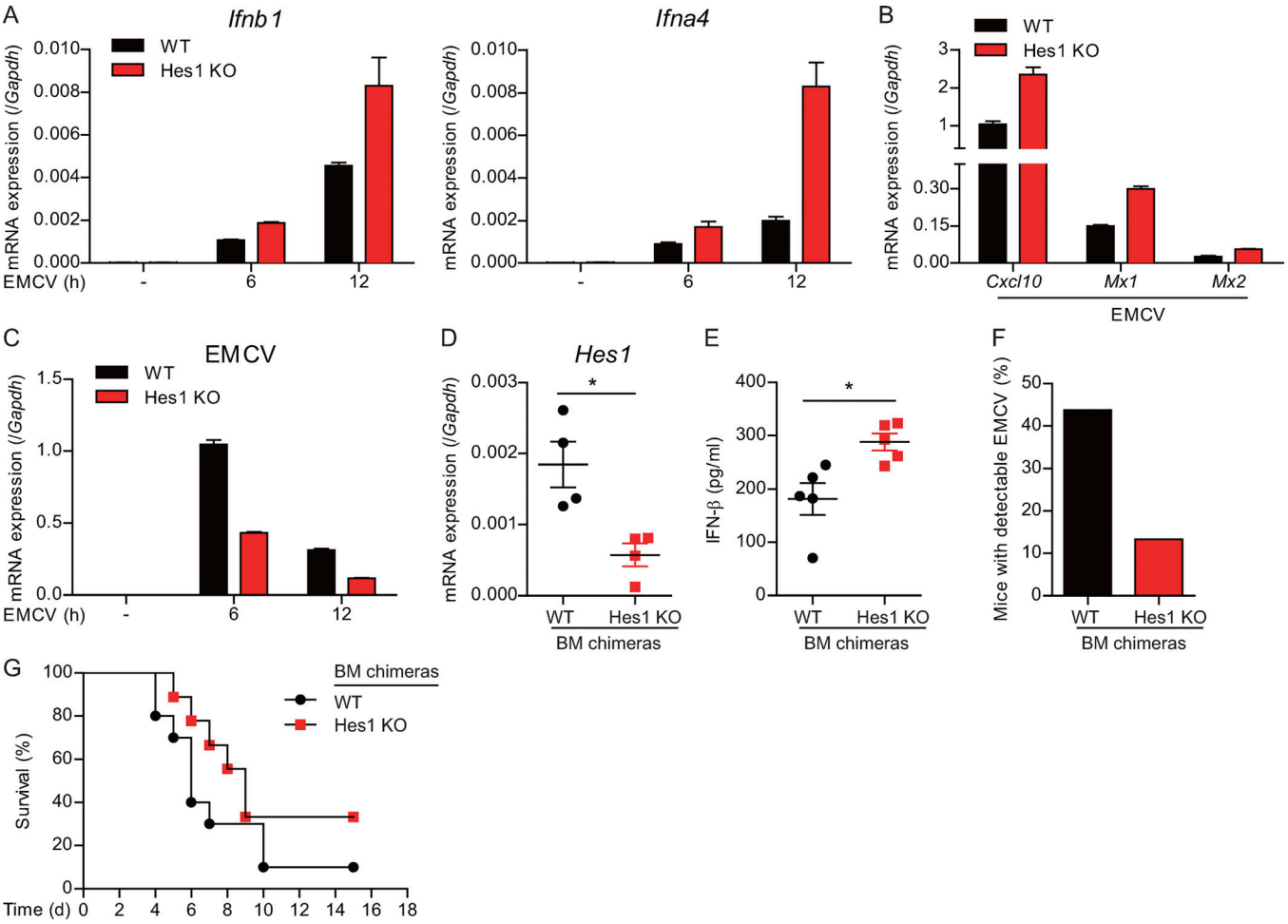

Figure 2. **Hes1 deficiency protects against EMCV infection in vitro and in vivo. (A)** qPCR analysis of *Ifnb1* and *Ifna4* in *Hes1*$^{+/+}$*Cre-ER*^{T2} (WT) and *Hes1*$^{fl/fl}$*Cre-ER*^{T2} (Hes1 KO) BMDMs infected with EMCV (MOI = 10) for the indicated periods. **(B and C)** qPCR analysis of ISGs (B) and EMCV replication (C) in WT and Hes1 KO BMDMs infected with EMCV (MOI = 10) for 6 h. **(D)** qPCR analysis of mRNA expression of *Hes1* in bone marrow cells from WT and Hes1 KO chimeric mice. **(E and F)** ELISA of IFN-β in serum (E) or percentage of mice with detectable EMCV in heart (F) of WT and Hes1 KO chimeric mice at day 4 after infection with a sublethal dose of EMCV (MOI = 5). **(G)** Survival rate of age-matched and sex-matched chimeras of WT (n = 10) and Hes1 KO (n = 9) infected with a lethal dose of EMCV (MOI = 6.6). Data are representative of two (A–C, E, and F; mean + SD of technical triplicates in A–C and mean ± SEM in E) or three (D and G; mean ± SEM in D) independent experiments. Each symbol represents an individual mouse. *, P < 0.05 (Student's t test).

higher than those of control mice (Fig. 2 E). Meanwhile, 44% of WT mice exhibited detectable EMCV in heart, while EMCV was detected only in 13% of Hes1-deficient mice at day 4 after infection (Fig. 2 F), indicating that Hes1 deficiency increased the ability of virus clearance in a host target organ. When infected with a lethal dose of EMCV, Hes1-deficient mice showed enhanced survival relative to WT mice (Fig. 2 G). Collectively, these findings demonstrated that in the context of viral infections, Hes1 acted as an endogenous brake of type I IFN production and thus host antiviral immunity.

Hes1 attenuates the IFN signature and lupus nephritis in vivo

Under homeostatic conditions, type I IFNs are constitutively produced at vanishingly low quantities yet are essential for maintaining immune balance (Gough et al., 2012). Having established that Hes1 negatively regulated expression of type I IFNs and ISGs under immune-activated conditions in vitro and in vivo, we next sought to determine whether Hes1-mediated suppression also occurred under homeostasis. qPCR analysis revealed that expression of *Ifnb1*, *Iigp1*, *Ccl12*, *Cxcl10*, and *Mx2* was significantly increased in Hes1-deficient resting peritoneal macrophages compared with WT cells (Fig. 3 A), indicating that Hes1 suppressed IFN and ISG expression at the basal level. It has been widely accepted that persistent type I IFN exposure and subsequent type I IFN signaling leading to ISG expression (referred to as the IFN signature) are characteristic features of SLE pathogenesis (Crow, 2014). We therefore investigated whether Hes1 deficiency contributed to the IFN signature in a 2,6,10,14-tetramethylpentadecane (TMPD)–induced murine model of lupus (Reeves et al., 2009). As expected, in WT mice, TMPD administration markedly induced the IFN signature, as evidenced by expression of ISGs such as *Ifit1*, *Cxcl10*, *Mx1*, and *Mx2*, in peritoneal cells (Fig. S2). Interestingly, Hes1-deficient mice exhibited a heightened TMPD-induced IFN signature compared with control animals (Fig. 3 B), demonstrating that Hes1 acts to attenuate the IFN signature in lupus-prone conditions. One

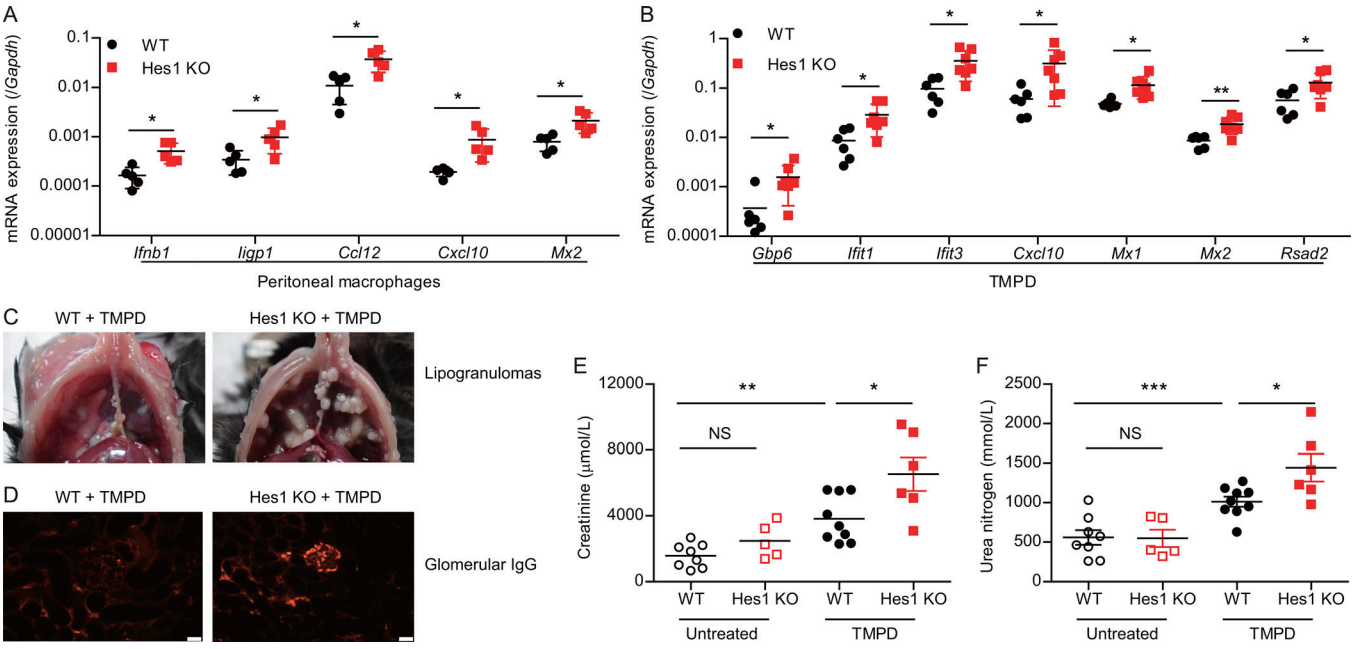

Figure 3. **Hes1 deficiency promotes the IFN signature and exacerbates lupus nephritis. (A)** qPCR analysis of *Ifnb1* and a subset of ISGs in peritoneal macrophages from *Hes1*$^{+/+}$*Cre-ER*^{T2} (WT, *n* = 5) and *Hes1*$^{fl/fl}$*Cre-ER*^{T2} (Hes1 KO, *n* = 5) mice. **(B)** qPCR analysis of ISGs in peritoneal cells from WT (*n* = 6) and Hes1 KO (*n* = 7) mice treated with TMPD (0.5 ml per mouse) for 2 wk. **(C and D)** Photographs of lipogranulomas in peritoneal cavity (C) or immunofluorescence of glomerular deposition of IgG in kidney (D) in WT and Hes1 KO mice 14 wk after TMPD treatment. **(E and F)** Quantitative analysis of creatinine (E) and urea nitrogen (F) in urine samples from untreated WT (*n* = 8) and Hes1 KO (*n* = 5) mice or from WT (*n* = 9) and Hes1 KO (*n* = 6) mice 14 wk after TMPD (0.5 ml per mouse) treatment. Scale bars, 20 µm. Data are representative of two (C and D) independent experiments or pooled from two (A, B, E, and F; mean ± SEM) independent experiments. Each symbol represents an individual mouse. *, P < 0.05; **, P < 0.01; ***, P < 0.001 (Student's *t* test).

prominent phenotype of the TMPD model is development of lipogranulomas adhering to the peritoneal mesothelial cell surface (Reeves et al., 2009), which was markedly exacerbated in Hes1 KO mice compared with WT controls (Fig. 3 C). Clinically evident lupus nephritis is one of the pathological features of SLE, which is characterized by glomerular immune complex deposition and results in accumulation of creatinine and urea nitrogen (Sprangers et al., 2012; Davidson, 2016). Therefore, we further investigated whether Hes1 deficiency affected development of TMPD-induced lupus nephritis. Hes1-deficient mice showed enhanced glomerular IgG deposition relative to that of WT mice (Fig. 3 D). While quantitative analysis of urine samples detected comparable baseline levels of creatinine and urea nitrogen in untreated WT and Hes1 KO mice, Hes1-deficient mice exhibited significantly increased levels of creatinine and urea nitrogen after TMPD treatment (Fig. 3, E and F), suggesting that Hes1 deficiency exacerbated renal disease severity. Collectively, these data implicated Hes1 as an endogenous suppressor of type I IFNs under homeostasis as well as autoimmune conditions.

Hes1 does not directly repress type I IFNs and ISGs

To gain mechanistic insights into Hes1-mediated suppression on IFNs, we investigated the effects of Hes1 in a luciferase assay system. Overexpression of Hes1 inhibited luciferase activities driven by a *Ifnb1* promoter in RAW 264.7 mouse macrophages under both poly(I:C) and LPS-stimulated conditions (Figs. 4 A and S3 A), suggesting that Hes1 overexpression was sufficient to suppress TLR-mediated induction of type I IFNs.

To confirm the above findings in the setting of endogenous IFN genes and delineate which domains of Hes1 were involved in Hes1-mediated suppression, we infected primary macrophages with retroviruses expressing WT full-length Hes1 (Hes1-FL) or Hes1 mutants harboring mutations or deletions of key functional domains (Kobayashi and Kageyama, 2014), including a dominant-negative mutant (dnHes1) that cannot bind DNA but can still dimerize with endogenous WT Hes1 to form a non–DNA-binding heterodimeric complex, a truncated Hes1 (Hes1ΔHLH) lacking the helix-loop-helix region that serves as a dimerization domain and a platform for interaction with additional proteins, and a truncated Hes1 (Hes1ΔWRPW) lacking the C-terminal WRPW motif (Trp-Arg-Pro-Trp) essential for recruiting corepressors such as transducing-like enhancer (TLE) proteins (Fig. 4 B). While infection of primary macrophages with WT Hes1-expressing virus efficiently blocked poly(I:C) and LPS induction of *Ifnb1* and ISGs such as *Ccl12* and *Mx1* (Figs. 4 C and S3 B), the suppressive effects of Hes1 were partially abolished upon mutating or deleting the key functional domains (Fig. 4 C). In particular, loss of the WRPW motif robustly and consistently reduced the suppressive capacity of Hes1 (Fig. 4 D), suggesting that WRPW motif–mediated recruitment of transcription corepressors may be important for the inhibitory action of Hes1.

To further explore the transcription regulatory mechanisms by Hes1, we determined genome-wide distribution of Hes1 protein by chromatin immunoprecipitation followed by deep sequencing (ChIP-seq) in primary macrophages. Prominent Hes1 occupancy was observed on a canonical Hes1 target gene

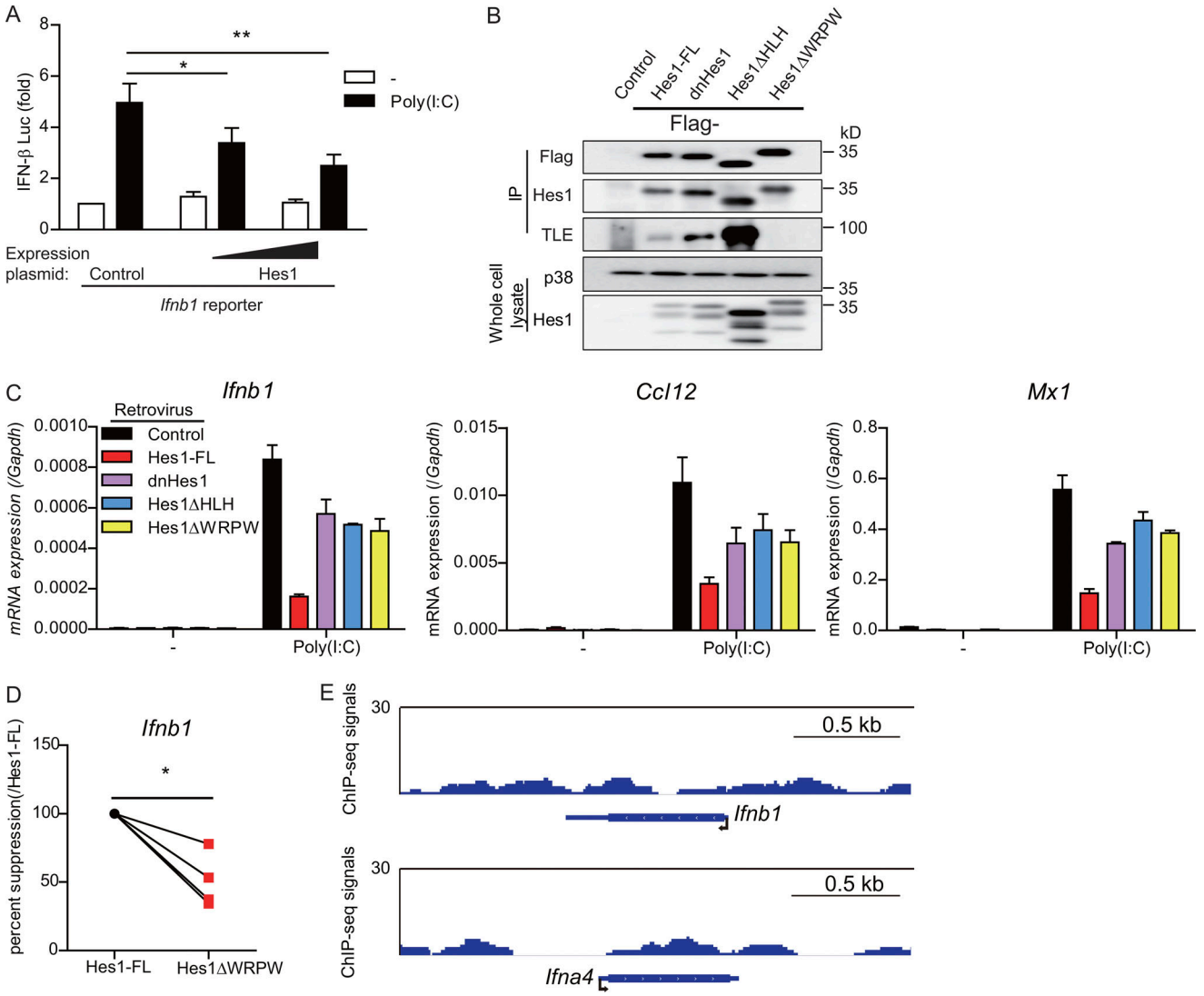

Figure 4. **Hes1 inhibits *Ifnb1* expression via its key functional domains. (A)** Luciferase activities in RAW 264.7 cells cotransfected with an *Ifnb1* promoter-driven reporter construct and a Hes1 expression plasmid or control empty vector. 18 h after transfection, cells were left untreated or stimulated with 10 µg/ml poly(I:C) for 8 h, and cell lysates were analyzed for luciferase activity. **(B)** Immunoblotting (IB) analysis of indicated proteins in immunoprecipitated (IP) samples and whole-cell lysates of HEK 293T cells that overexpressed WT Hes1 or Hes1 mutants. **(C)** qPCR analysis of *Ifnb1* and related genes (*Ccl12* and *Mx1*) in WT BMDMs transduced with control retroviruses or retroviruses expressing Hes1 or Hes1 mutants, subsequently with or without 1 µg/ml poly(I:C) stimulation for 3 h. **(D)** Percent suppression of *Ifnb1* in BMDMs expressing Hes1ΔWRPW relative to results obtained for cells expressing Hes1-FL (set as 100). Cells were stimulated with poly(I:C) for 1 h. **(E)** ChIP-seq analysis of Hes1 occupancy along gene loci of *Ifnb1* (top) and *Ifna4* (bottom) in BMDMs. Data are representative of one (E), two (B), or three (C; mean + SD of technical triplicates) independent experiments or pooled from three independent experiments (A and D; mean + SD in A). *, P < 0.05; **, P < 0.01 (Student's *t* test).

Ascl1 (*Mash1*) and Hes1 acted to suppress *Ascl1* as expected (Fig. S3 C). However, we did not identify notable Hes1 binding peaks in the gene loci of *Ifnb1*, *Ifna4* (Fig. 4 E), and ISGs such as *Mx1*, *Mx2*, and *Ccl12* (Fig. S3 D), indicating that type I IFN genes were not the direct transcriptional targets of Hes1. Taken together, these findings supported that Hes1 negatively regulated expression of type I IFNs via mechanisms other than direct transcription repression.

Hes1 inhibits TLR signaling leading to IFN expression

As the above genomic analysis excluded the possibility of direct regulation of IFNs and ISGs by Hes1, we hypothesized that Hes1 indirectly modulated expression and/or activities of key transcription factors responsible for IFN production. NF-κB and IRF family transcription factors are the major drivers of type I IFN expression downstream of TLR3 (Honda et al., 2006). Hes1 deficiency did not alter TLR3-mediated activation of canonical NF-κB signaling as measured by p65 phosphorylation and IκBα degradation (Fig. 5 A; signal intensities are quantitated in Fig. S4 A). In contrast, upon poly(I:C) stimulation, Hes1-deficient macrophages showed enhanced serine phosphorylation of IRF3, a hallmark of its transcriptional activation capacity, relative to WT cells whereas total IRF3 protein levels were comparable (Fig. 5 B and S4 A), suggesting that Hes1 targets signaling events

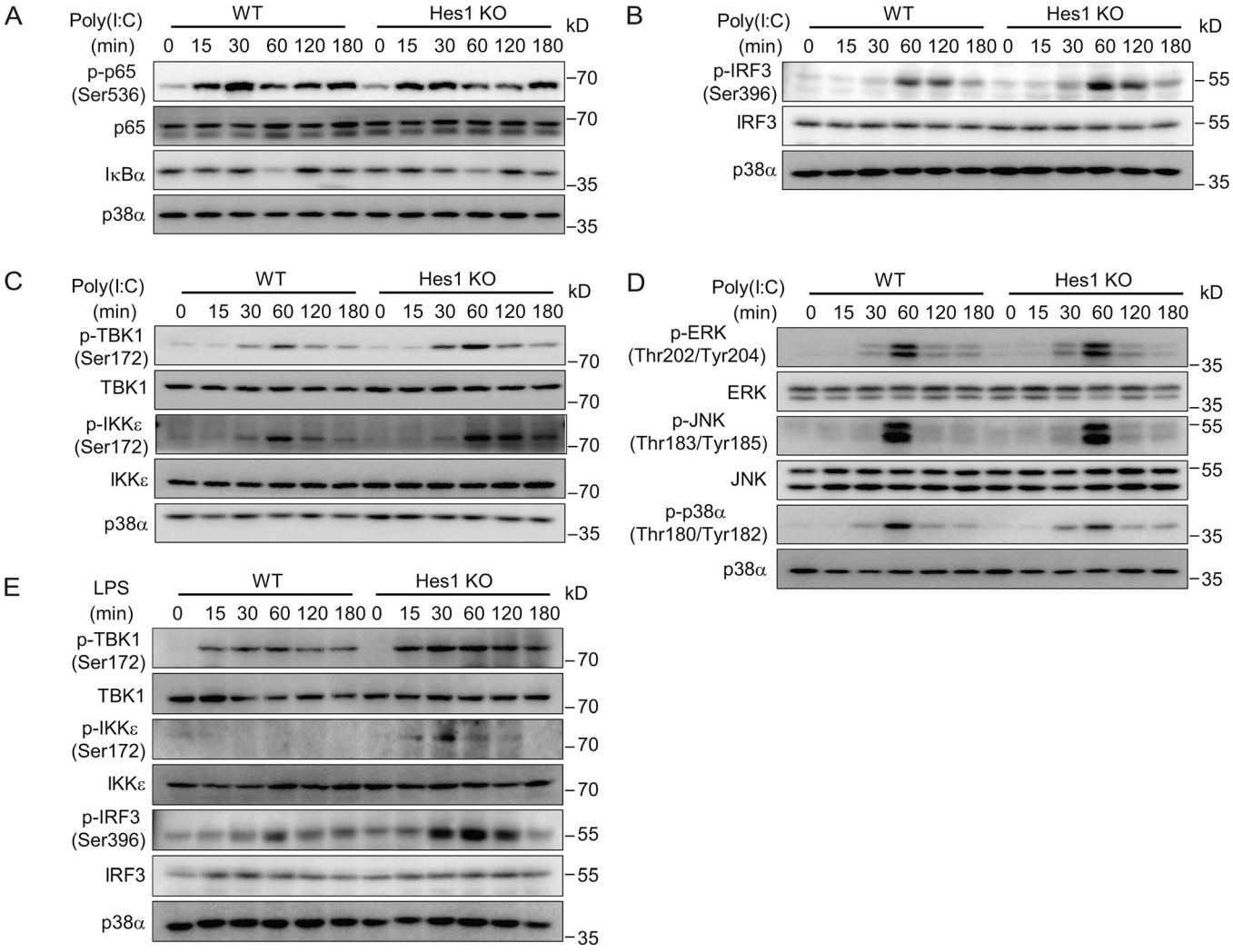

Figure 5. **Hes1 inhibits activation of TLR–IRF3 signaling cascades. (A–D)** Immunoblotting analysis of phosphorylated (Ser536) and total p65 and total IκBα (A); phosphorylated (Ser396) and total IRF3 (B); phosphorylated (Ser172) and total TBK1 and IKKε (C); and phosphorylated (Thr202/Tyr204, Thr183/Tyr185, and Thr180/Tyr182) and total ERK, JNK, and p38α (D) in whole-cell lysates of BMDMs obtained from *Hes1*$^{+/+}$*Cre-ER*^{T2} (WT) and *Hes1*$^{fl/fl}$*Cre-ER*^{T2} (Hes1 KO) mice and treated for various times (above lanes) with poly(I:C) (1 µg/ml). **(E)** Immunoblotting analysis of phosphorylated and total TBK1, IKKε, and IRF3 in whole cell lysates of WT and Hes1 KO BMDMs treated with LPS (10 ng/ml) for various times. Data are representative of three independent experiments (A–E).

upstream of IRF3. Phosphorylation of IRF3 is dependent on activation of two IκB kinase (IKK)–related kinases, TANK-binding kinase 1 (TBK1) and IKKε, downstream of TLR3 (Kawai and Akira, 2011; Ikushima et al., 2013). Interestingly, Hes1 deficiency promoted phosphorylation and thus activation of the IRF3 upstream kinases TBK1 and IKKε without altering activation and/or expression of other key signaling molecules such as ERK/JNK/p38α MAPKs (Fig. 5, C and D; and Fig. S4 A). Similarly, enhanced phosphorylation of TBK1, IKKε, and IRF3 was also observed in Hes1-deficient macrophages in response to LPS stimulation (Fig. 5 E; signal intensities are quantitated in Fig. S4 B). Together, these results demonstrated that Hes1 suppressed activation of IFN-inducing key transcription factor IRF3 by targeting TLR upstream signaling components.

Hes1 suppresses Wdfy1 to regulate IFN expression

Next, we sought to investigate the mechanisms underlying Hes1-mediated inhibition of TLR3 upstream signaling. Given that Hes1, a transcription factor, attenuated activation of TBK1 and IKKε acutely as early as 30 min after stimulation (Fig. 5 A), we postulated that Hes1 likely modulated expression of signaling molecules upstream of TBK1 and IKKε. Nevertheless, Hes1 did not affect expression of well-characterized TLR3 key signaling proteins, including TNF receptor–associated factor (TRAF) 3 and TRIF (Fig. S4 C). Therefore, we further analyzed the Hes1 KO RNA-seq dataset for differentially expressed genes that may explain the signaling phenotypes and found that among genes up-regulated in Hes1-deficient macrophages was *Wdfy1* (Fig. 6 A), encoding an adaptor protein that facilitates recruitment of TRIF to TLR3 and TLR4 (Hu et al., 2015). The increase of *Wdfy1* gene expression in Hes1-deficient BMDMs was confirmed by qPCR in multiple independent experiments (Fig. 6 B). Notably, inhibition of Wdfy1 expression by Hes1 was independent of the cellular stimulation status and already apparent at baseline, as shown by assessment of both mRNA and protein levels (Fig. 6, B and C). Moreover, an increase in Wdfy1 was also observed

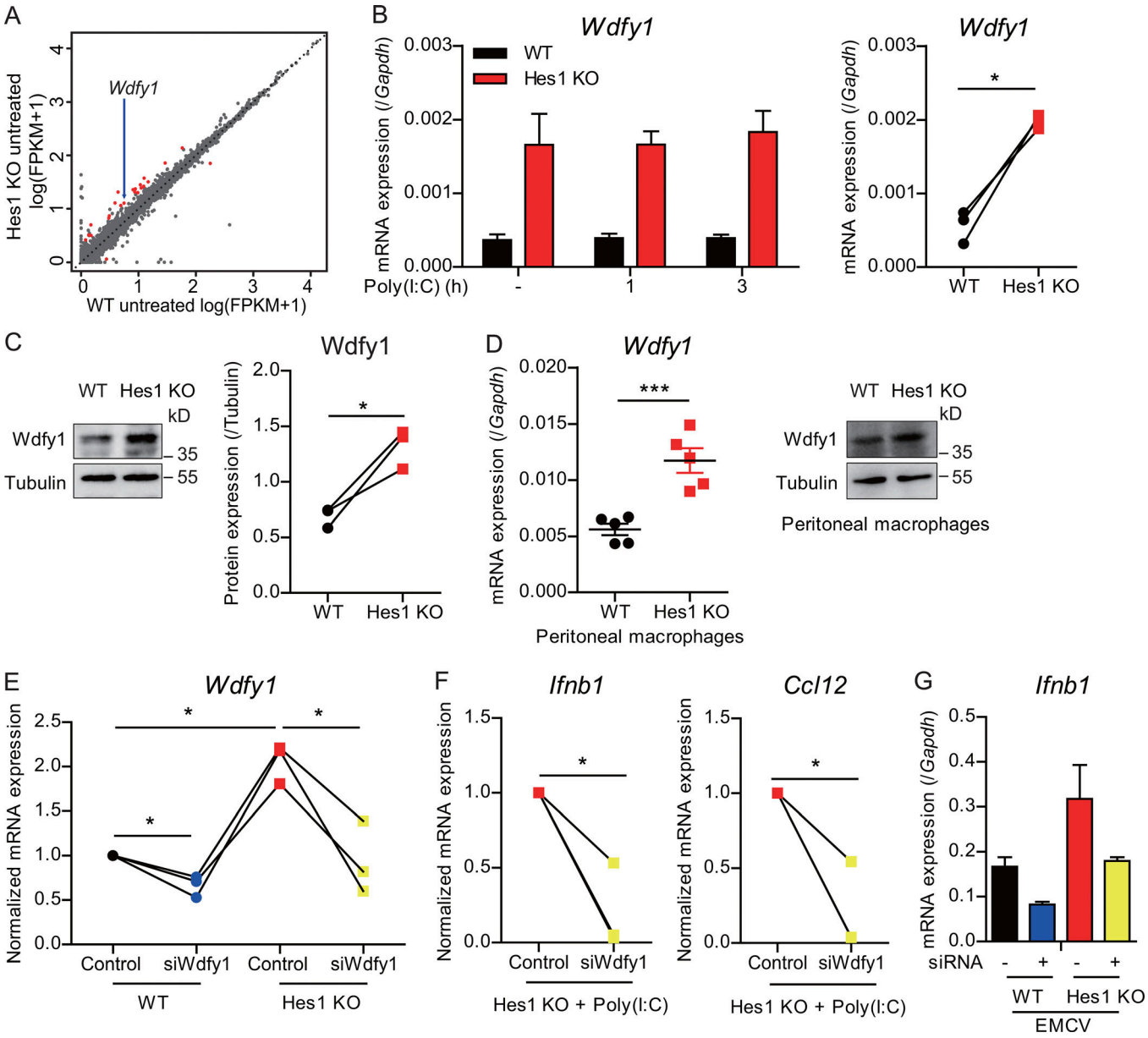

Figure 6. **Hes1 represses Wdfy1 expression to regulate TLR-induced IFNs. (A)** Scatter blot of RNA-seq analysis of differentially expressed genes in *Hes1*$^{+/+}$*Cre-ER*^{T2} (WT) and *Hes1*$^{fl/fl}$*Cre-ER*^{T2} (Hes1 KO) BMDMs at basal levels. *Wdfy1* was marked with an arrow. **(B)** qPCR analysis of Wdfy1 mRNA in WT and Hes1 KO BMDMs stimulated with 1 µg/ml poly(I:C) (left) for indicated periods (horizontal axes), and cumulative results for induction of *Wdfy1* in WT and Hes1 KO cells under unstimulated condition (right). **(C)** Immunoblotting analysis of protein expression of Wdfy1 in resting WT and Hes1 KO BMDMs (left) and cumulative results of Wdfy1 expression were shown as in right. Levels of tubulin served as loading controls. **(D)** qPCR analysis of Wdfy1 mRNA expression (left) and immunoblotting analysis of Wdfy1 protein levels (right) in peritoneal macrophages from WT and Hes1 KO mice. **(E–G)** qPCR analysis of *Wdfy1*, *Ifnb1*, or ISG expression in BMDMs from indicated mice transfected with siWdfy1 or control siRNA. Cells were without (E) or with poly(I:C) stimulation for 1 h (F) or with EMCV infection for 6 h (G). Data are representative of one (A) or three (B [left], C [left], D [right], and G; mean + SD of technical triplicates in B [left] and G) independent experiments or pooled from three (B [right], C [right], E, and F) or five (D [left]; mean ± SEM) independent experiments. Each symbol represents an individual mouse. *, P < 0.05; ***, P < 0.001 (Student's *t* test).

in vivo in resident peritoneal macrophages from Hes1-deficient animals (Fig. 6 D). Taken together, these data demonstrated that Hes1 reduced macrophage *Wdfy1* gene expression in vitro and in vivo.

To evaluate whether changes of *Wdfy1* were causally related to Hes1-regulated IFN expression, we knocked down *Wdfy1* in Hes1-deficient primary macrophages using RNA interference (Fig. 6 E). While siRNA oligo transfection specifically decreased *Wdfy1* expression in Hes1 KO BMDMs, compared with control nontargeting siRNA oligos, *Wdfy1* knockdown did not significantly alter cell viability, as assessed by absolute cell counts as well as cell death assays (Fig. S4, D and E). Importantly, diminishing *Wdfy1* expression reduced *Ifnb1* and ISG mRNA levels in Hes1-deficient cells in response to poly(I:C) stimulation as well as EMCV infection (Fig. 6, F and G), implying that Hes1 deficiency–associated *Wdfy1* up-regulation contributed to the

IFN overproduction phenotype. To further determine the physiological function of Wdfy1 in vivo, we adoptively transferred control siRNA or *Wdfy1* siRNA-transfected macrophages into WT recipients and found that both control and *Wdfy1* knocked down cells could be faithfully recovered from the peritoneal cavity, certifying that Wdfy1 loss of function did not affect survival of transferred cells and thus did not interfere with the adoptive transfer process (Fig. S4 F). Consistent with the in vitro observations, reducing *Wdfy1* expression in Hes1-deficient macrophages attenuated the TMPD-induced IFN signature in vivo (Fig. S4 G). Moreover, adoptive transfer of Wdfy1-overexpressed macrophages protected mice from a lethal dose of EMCV infection, mimicking the phenotypes of the Hes1-deficient animals (Fig. S4, H and I). Together, these findings suggested that Hes1 limited type I IFN–mediated responses via suppression of an adaptor molecule Wdfy1 in vitro and in vivo.

Vegfc serves as a direct transcriptional target of Hes1-regulated IFN production

To gain further insights into the mechanisms of Hes1-imposed regulation on *Wdfy1*, we assessed whether Hes1 directly bound the endogenous *Wdfy1* gene locus in primary macrophages using the Hes1 ChIP-seq dataset. Among the identified 5,819 Hes1 binding peaks, >40% of these peaks were located in the gene promoter regions (Fig. 7 A) with binding motifs enriched for canonical target sequences such as E boxes (Fig. S5 A), validating the reliability of the dataset. Unexpectedly, we did not find any prominent Hes1-binding peaks in the promoter region or the gene body region of the *Wdfy1* locus (Fig. 7 B), indicating that *Wdfy1* was not the direct transcriptional target of Hes1. Instead, we located a distinct binding peak of Hes1 near the promoter region of the *Vegfc* gene locus (Fig. 7 C), suggesting a direct regulation of the growth factor–encoding *Vegfc* gene by Hes1. Interestingly, VEGF-C has been reported to inhibit WDFY1 expression in cancer cells (Stanton et al., 2013; Dutta et al., 2016). These lines of evidence prompted us to hypothesize that Hes1 suppressed *Wdfy1* expression through regulation of *Vegfc* and to examine expression of *Vegfc* in Hes1-deficient macrophages. We found that *Vegfc* expression was consistently down-regulated in Hes1-deficient BMDMs (Fig. 7 D), suggesting that Hes1 might promote *Vegfc* expression via binding to its promoter region. Indeed, overexpression of Hes1 enhanced luciferase activities driven by the *Vegfc* promoter, in which two of the three putative E boxes played a critical role (Fig. 7 C and E), further supporting the notion that Hes1 acted as a positive regulator of *Vegfc* expression. To functionally connect Hes1-regulated VEGF-C with the changes of IFNs, we overexpressed Vegfc in Hes1-deficient BMDMs via viral transduction. In Hes1-deficient cells, forced expression of Vegfc decreased *Wdfy1* expression to a comparable level to that of WT cells (Fig. 7 F), with a concomitant reduction of *Ifnb1* and *Mx1* expression (Fig. 7 G), functionally implicating VEGF-C in the Hes1–WDFY1–IFN regulatory loop. To extend the functional link between Hes1 and VEGF-C to in vivo settings, Hes1-deficient animals were administrated with recombinant murine VEGF-C in TMPD treatment and viral infection models. In the Hes1-deficient background, VEGF-C administration attenuated heightened Wdfy1 expression and the IFN signature (Fig. 7 H) and compromised the host defense against EMCV infection (Fig. 7 I), underscoring VEGF-C as a key functional target of Hes1 in regulation of IFN-mediated immune responses. In summary, these findings indicated that Hes1 promoted *Vegfc* transcription to suppress WDFY1–IFN expression and subsequently attenuated IFN-mediated host defense and autoimmune processes.

Discussion

Production of inflammatory mediators and key immune effector molecules is negatively controlled by multiple mechanisms at virtually every step of the production process to prevent toxicity and maintain immune homeostasis (Porritt and Hertzog, 2015). We have previously reported that the canonical Notch target Hes1 selectively inhibits expression of inflammatory cytokines and chemokines via targeting the gene transcription initiation or elongation step in macrophages, which serves as a crucial negative regulatory mechanism of TLR-induced inflammatory responses (Hu et al., 2008; Shang et al., 2016a). However, whether Hes1 regulates TLR-induced production of type I IFNs remains unclear. Here, we demonstrated that Hes1 suppressed TLR3/4-mediated expression of type I IFNs and downstream ISGs in macrophages without directly affecting gene transcription of IFNs and ISGs or activation of TLR-mediated canonical events such as NF-κB and MAPKs. Instead, Hes1 inhibited activation of IRF3 via suppression of mRNA expression of Wdfy1, an adaptor molecule facilitating activation of the signaling cascade upstream of IRF3 (Hu et al., 2015). Furthermore, Hes1 inhibited Wdfy1 expression through direct binding to the *Vegfc* gene locus and promoting expression of VEGF-C, which negatively regulates *Wdfy1* transcription (Stanton et al., 2013). Our findings thus implicate that Hes1 plays a critical role in restraining type I IFN production via an unusual mechanism by targeting VEGF-C that may act in an autocrine or paracrine fashion to limit WDFY1 expression and thus type I IFN production (Fig. S5 B). As a result, Hes1 attenuated the host antiviral defense and development of lupus-associated symptoms, two processes in which type I IFNs were indispensable. Hence, the insights gained from this study advanced our understanding of the (patho)physiological function of Hes1 in immune regulation with potential therapeutic implications for viral infections and autoimmune diseases. Investigating the role of Hes1 is particularly relevant for human disease settings, as TLR stimulation strongly promotes expression of Notch target genes, including Hes1 in primary human monocytes and macrophages. Although the exact biological significance of such up-regulation in human cells remains obscure and represents an interesting topic for future research, this study may suggest that the homeostatic negative function described here in the mouse system may also be in effect in humans.

Hes1 generally represses target gene expression via binding to sequence-specific DNA elements such as N box and/or E box (Kobayashi and Kageyama, 2014). In addition, Hes1 also inhibits gene transcription via attenuation of polymerase II–mediated productive elongation by antagonizing recruitment of a positive transcription elongation factor complex, P-TEFb (Shang et al.,

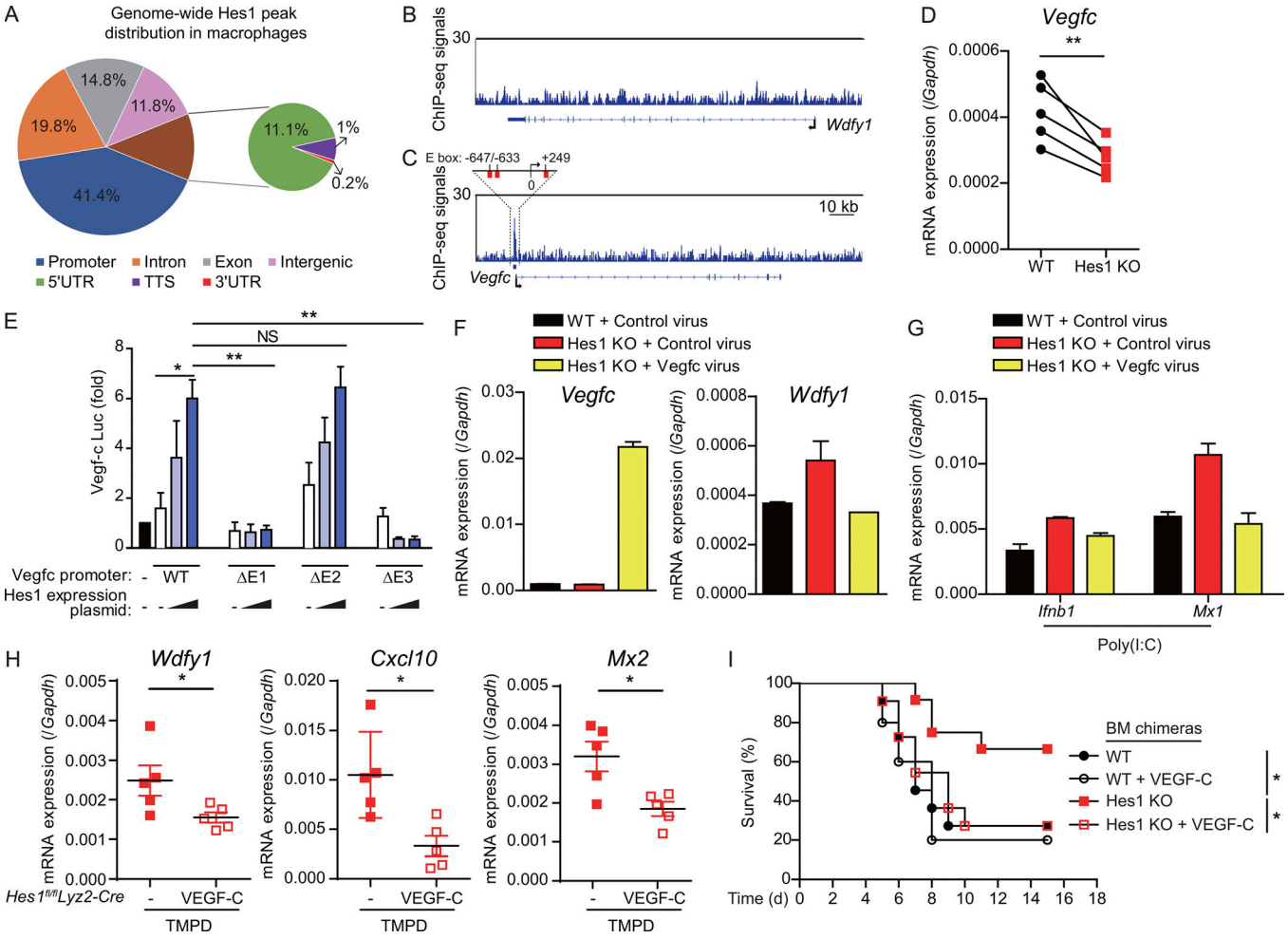

Figure 7. **Hes1 promotes *Vegfc* transcription to suppress Wdfy1 expression. (A)** Genome-wide analysis of Hes1 binding peak distribution in gene loci in unstimulated BMDMs. UTR, untranslated region; TTS, transcription termination site. **(B and C)** ChIP-seq analysis of Hes1 occupancy along gene loci of *Wdfy1* (B) and *Vegfc* (C) in macrophages. **(D)** qPCR analysis of *Vegfc* expression in $Hes1^{+/+}$*Cre-ER*^{T2} (WT) and $Hes1^{fl/fl}$*Cre-ER*^{T2} (Hes1 KO) BMDMs. **(E)** Luciferase activities in CMT93 cells cotransfected with WT or E box mutant *Vegfc* promoter-driven reporter constructs and a Hes1 expression plasmid or control empty vector. 18 h after transfection, cell lysates were analyzed for luciferase activity. **(F and G)** qPCR analysis of *Vegfc* and *Wdfy1* expression in WT or Hes1 KO BMDMs transduced with control or Vegfc-expressing (yellow bar) virus in the unstimulated condition (F) or *Ifnb1* and *Mx1* expression in these cells stimulated with poly(I:C) for 1 h (G). **(H)** qPCR analysis of *Wdfy1*, *Cxcl10*, and *Mx2* in peritoneal cells from $Hes1^{fl/fl}$*Lyz2-Cre* mice treated with TMPD for 7 d with or without VEGF-C pretreatment. **(I)** Survival of WT and Hes1 KO chimeras infected with EMCV with or without VEGF-C pretreatment (WT and Hes1 KO + VEGF-C, n = 11; WT + VEGF-C, n = 5, Hes1 KO, n = 12). Data are representative of one experiment (A–C) or three (F and G; mean + SD of technical triplicates) independent experiments or pooled from two (H and I; mean ± SEM in H), three (E; mean + SD), or five (D) independent experiments. Each symbol represents an individual mouse. *, P < 0.05; **, P < 0.01 (Student's *t* test or log-rank test in I).

2016a). Although predominantly viewed as a transcription repressor, it has been described that Hes1 could function as a transcription activator under certain circumstances. For example, Hes1 could be switched from a transcriptional repressor to a transcriptional activator to induce development-related gene expression for neuronal differentiation (Ju et al., 2004). Consistent with this notion, we found that Hes1 was physically located on the *Vegfc* gene locus and promoted *Vegfc* gene expression. Of note, in macrophages, transcriptional activation by Hes1 is an exception rather than a rule, as Hes1-suppressed genes significantly outnumbered Hes1-activated genes (Fig. 6 A). Therefore, our findings, for the first time, show that Hes1 functions as a novel negative regulator of IFN responses via an unusual mechanism of enhancing expression of the soluble factor VEGF-C, which is mechanistically distinct from the previous studies by us and others depicting Hes1's action (Hu et al., 2008; Kobayashi and Kageyama, 2014; Shang et al., 2016a). Molecular mechanisms underlying transcriptional activation properties of Hes1 are poorly understood and will be an interesting subject for future investigation, especially in the context of inflammatory responses.

To mediate gene repression, Hes1 interacts with TLE corepressors in a manner dependent on its C-terminal WRPW domain (Fisher et al., 1996). The mammalian TLE family proteins are homologous to *Drosophila melanogaster* Groucho protein and have been mainly implicated in developmental processes (Buscarlet and Stifani, 2007). Interestingly, Hes1 seemed to inhibit IFN responses through recruitment of its corepressor,

TLE, as a Hes1 mutant with deletion of the WRPW domain lost the capacity to suppress expression of type I IFNs. Similar to Hes1, little is known about function of TLE family proteins in the immune system. TLE1 has been implicated in the negative regulation of inflammatory responses (Alvarez et al., 2011; Ramasamy et al., 2016), although the exact mechanisms of action are unclear. Further studies will be needed to clarify how Hes1 cooperates with TLE family members to regulate gene expression during immune responses (Zhang et al., 2019).

The function of WDFY1 remains obscure, especially in the immune system. Recent studies identified WDFY1 as a positive regulator of TLR3/4 signaling, suggesting a new function of WDFY1 in regulation of innate immune responses (Hu et al., 2015; Nandakumar and Paludan, 2015). Although studies have found that transcription of WDFY1 is controlled by the VEGF-C–NRP2 axis in cancer cells (Stanton et al., 2013), it remains unclear how WDFY1 expression is regulated in immune cells. Notably, expression of VEGF-C and its receptor, VEGFR-3, is substantially increased in primary macrophages upon bacterial infections or stimulation with TLR agonists. The enhanced VEGF-C–VEGFR3 signaling then restrains TLR4-mediated inflammatory responses, which represents a negative feedback mechanism by which immune cells avoid "overreaction" during bacterial infection (Zhang et al., 2014). In addition to ligation with VEGFR3, VEGF-C also binds to its nontyrosine kinase receptor, NRP2, to regulate autophagy and endocytic trafficking in cancer cells by suppressing transcription of the downstream effector gene WDFY1 (Stanton et al., 2013; Dutta et al., 2016). Here, our findings supported that VEGF-C–WDFY1 signaling was likely involved in IFN responses and that Hes1 may modulate crosstalk between VEGF-C-WDFY1 and TLR signaling to fine-tune IFN expression.

Materials and methods

Mice

The experiments using mice were approved by the Institutional Animal Care and Use Committees at Tsinghua University. *Hes1*$^{fl/fl}$ mice were originally obtained from R. Kageyama (Kyoto University, Kyoto, Japan). Mice with inducible deletion of Hes1 (*Hes1*$^{fl/fl}$*Cre-ER*^{T2}) were generated by crossbreeding *Hes1*$^{fl/fl}$ animals with *Cre-ER*^{T2} mice on the C57BL/6J background. Deletion of Hes1 was induced by i.p. injection with 2 mg per mouse of tamoxifen (T5648; Sigma-Aldrich) five times in 5 d. WT littermates were also injected with tamoxifen with the same dosage. Mice were used for experiments 7 d after tamoxifen administration. Mice with a myeloid-specific deletion of Hes1 (*Hes1*$^{fl/fl}$*Lyz2-Cre*) were generated by crossing *Hes1*$^{fl/fl}$ animals to *Lyz2-Cre* mice, and littermates with genotype of *Hes1*$^{fl/fl}$*Lyz2-Cre* and *Hes1*$^{+/+}$*Lyz2-Cre* were used for experiments. Experiments on mice were performed at 8–10 wk of age with gender-matched littermates. Bone marrow chimeras were generated as previously described (Hu et al., 2008). Briefly, *Hes1*$^{fl/fl}$*Cre-ER*^{T2} or *Hes1*$^{+/+}$*Cre-ER*^{T2} mice were i.p. injected with 2 mg per mouse of tamoxifen five times within 5 d. 7 d after tamoxifen treatment, 10^6 bone marrow cells from *Hes1*$^{fl/fl}$*Cre-ER*^{T2} or *Hes1*$^{+/+}$*Cre-ER*^{T2} mice were intravenously injected into 6-wk-old irradiated (one dose of 11 Gy) C57BL/6J recipient mice. Chimeric mice were used for experiments 6 wk after bone marrow reconstitution.

TMPD-induced IFN signature and nephritis

The IFN signature was induced by i.p. injection of 0.5 ml TMPD (P9622; Sigma-Aldrich) in 12-wk-old *Hes1*$^{fl/fl}$*Cre-ER*^{T2} or *Hes1*$^{+/+}$*Cre-ER*^{T2} mice. Control mice received 0.5 ml mineral oil (M5310; Sigma-Aldrich) or PBS at the same time. 2 wk after injection, mice were euthanized by carbon dioxide exposure, and peritoneal cavities were washed with 5 ml PBS containing 2 mM EDTA. Total peritoneal cells were then harvested and used for the following experiments. For TMPD-induced nephritis, *Hes1*$^{fl/fl}$*Cre-ER*^{T2} or *Hes1*$^{+/+}$*Cre-ER*^{T2} mice were given TMPD by i.p. injection (0.5 ml per mouse) for 14 wk. The urine of experimental animals was then collected for creatinine and urea nitrogen analysis using a creatinine assay kit (ab65340; Abcam) and urea nitrogen detection kit (KT-747; KAMIYA) according to the manufacturer's instructions, respectively. For the TMPD-induced IFN signature in the adoptive transfer experiments, total peritoneal cells were harvested 1 wk after TMPD administration. For VEGF-C–related experiments, 1 µg recombinant murine VEGF-C per mouse (268–10325; RayBiotech) was given via i.p. injection 24 h before TMPD treatment. 1 wk after TMPD administration, total peritoneal cells were harvested for gene expression analysis.

Adoptive transfer of macrophages

Macrophage adoptive transfer was performed as described previously (Shang et al., 2016a), with minor modifications. Briefly, BMDMs from *Hes1*$^{fl/fl}$*Cre-ER*^{T2} or *Hes1*$^{+/+}$*Cre-ER*^{T2}, Wdfy1-overexpessed BMDMs, Hes1-deficient BMDMs with Wdfy1 knockdown, or control cells were washed three times with PBS, and cell numbers were adjusted to 4×10^6 cells/ml in sterile PBS. A 500-µl suspension of BMDMs (2×10^6 cells) was injected i.p. into WT C57BL/6J mice. Mice were used for subsequent experiments 24 h after cell transfer.

EMCV infection

The EMCV strain (BJC3) originally isolated from porcine sources was kindly provided by Dr. Hanchun Yang (China Agricultural University, Beijing, China), and a series of virus titers were tested to obtain the optimal multiplicity of infection (MOI) for experimentation. For in vitro viral infection, BMDMs were infected with EMCV (MOI = 10) for indicated times. For in vivo infection, chimeric mice were i.p. injected with a sublethal dose of EMCV (MOI = 5) for 4 d to detect serum IFN-β and tissue viral titers. For the survival rate assay, mice were infected with a lethal dose of EMCV (MOI = 6.6) via i.p. injection. For VEGF-C–related experiments, mice were i.p. injected with recombinant murine VEGF-C (1 µg per mouse) for 24 h before EMCV infection.

Cell culture and stimuli

Murine BMDMs were obtained as previously described (Hu et al., 2008) and maintained in DMEM supplemented with 10% FBS (Gibco) and 10% L929 cell supernatant as conditioned medium providing macrophage colony-stimulating factor. Cell

culture–grade poly(I:C) (high molecular weight) was purchased from Invivogen, and LPS (*Escherichia coli* 0111: B4) was purchased from Sigma-Aldrich. IFNAR1 blocking antibody (AF3039) was purchased from R&D Systems.

Flow cytometry

For cell viability, BMDMs were washed with PBS 72 h after siRNA transfection and collected for counting cell number with trypan blue staining. Cell death was analyzed using an Annexin V Apoptosis Detection Kit (88–8007-72; eBioscience) according to the manufacturer's instructions. For the adoptive transfer experiments, 18 h after cell transfer, peritoneal cells from CD45.1 mice were collected and stained with APC/Cy7 anti-mouse CD45 (1:400, 103116; BioLegend), Brilliant Violet 421 anti-mouse CD45.1 (1:400, 110732; BioLegend), and PE/Cy7 anti-mouse CD45.2 (1:400, 25–0454-80; eBioscience) for identification of transferred macrophages. Cells were analyzed on an LSR Fortessa flow cytometer (BD Biosciences) using FlowJo software (BD Biosciences).

Immunofluorescence

Kidneys were fixed in 4% paraformaldehyde solution overnight and frozen in Tissue-Tek Embedding Medium (SAKURA) after dehydration in 30% sucrose solution. 10-µm sections were cut, and glomerular IgG was detected with DyLight*549-conjugated horse anti-mouse IgG (DI-2549; Vector Laboratories).

Reverse transcription and qPCR

RNA was extracted from whole-cell lysates with a total RNA purification Kit (GeneMarkbio) and reversely transcribed to cDNA with a PrimeScript RT Reagent Kit with gDNA Eraser (Perfect Real Time; Takara). qPCR was performed in triplicate determinants with an ABI StepOne Plus thermal cycler. Threshold cycle numbers were normalized to triplicate samples amplified with primers specific for *Gapdh*. qPCR primer sequences are listed in Table S1.

Isolation of resident peritoneal macrophages

Resident peritoneal macrophages were prepared as previously described (Shang et al., 2016a). Briefly, peritoneal exudate cells were washed out with ice-cold PBS containing 2 mM EDTA. After washing twice with PBS, peritoneal cells were resuspended in DMEM supplement with 10% FBS. The cells were then allowed to adhere for overnight in Petri dishes at 37°C. Nonadherent cells are removed by gently washing three times with warm PBS. The adherent cells were used as peritoneal macrophages.

RNA-seq analysis

For RNA-seq analysis, BMDMs from $Hes1^{fl/fl}Cre\text{-}ER^{T2}$ mice and $Hes1^{+/+}Cre\text{-}ER^{T2}$ mice were left untreated or stimulated with 1 µg/ml poly(I:C) for 1 or 3 h. Cells were then harvested for total RNA extraction with a total RNA purification kit (GeneMarkbio), and RNA was converted into RNA-seq quantification libraries (low-input library; 200 ng). RNA-seq libraries were sequenced with the pair-end option using an Illumina-HiSeq2500 Sequencer at BGI China per the manufacturer's recommended protocol. Pair-end RNA-seq reads were aligned to mouse genome mm10 using TopHat 2.1.0 with the parameters -i 70 -g 1 --no-novel-indels --coverage-search, and only uniquely mapped reads were preserved. For coverage of mapped RNA-seq reads in transcripts, the expression level of each genes transcripts was calculated as the normalized fragment count to fragment coverage for each transcript (per 1 kb) in per million fragments (FPKM). Differential expression analysis of genes between experimental conditions was implemented using the Cuff-diff program in Cufflinks 2.2.1. Genes with a P value <0.05 and (FPKM + 1) fold change ≥2 between two conditions were regarded as significantly up-regulated genes, and significantly down-regulated genes were identified with P value <0.05 and (FPKM + 1) fold changes ≤0.5 between two conditions. The RNA-seq data reported in this paper have been deposited in the Gene Expression Omnibus with the accession number GSE111169.

ELISA

IFN-β secretion was quantified by using paired anti-mouse IFN-β antibodies (capture antibody, 22400–1; detection antibody, 32401–1; PBL) according to the manufacturers' instructions. Mouse IFN-β (12405–1; PBL) was used as protein standard.

Dual-luciferase reporter assay

Murine *Ifnb1* reporter plasmid was constructed by subcloning 110 bp of the *Ifnb1* promoter into a luciferase expression vector (Seth et al., 2005). RAW 264.7 cells were cotransfected in duplicates with the IFN-β reporter plasmid and an expression plasmid (pCMV6-XL4-Hes1) encoding mouse Hes1 or a control vector (pCMV6-XL4) using Lipofectamine LTX with PLUS Reagent (Thermo Fisher). 18 h after transfection, cells were stimulated with poly(I:C) (10 µg/ml) or LPS (100 ng/ml) for 8 h, and cell lysates were prepared and analyzed using the Dual-Luciferase Report Assay System (Promega). Total protein concentration analyzed by using Pierce BCA Protein Assay Kit (Thermo Fisher) was used as an internal control. For luciferase assay in CMT93 cells, the murine *Vegfc* promoter sequence from position −700 to +500 bp was cloned into the pGL3-Basic reporter plasmid (pGL3-Basic-*Vegfc*). *Vegfc* promoter E box mutations were generated by deleting E box of E1 (CAGCTG, −647 bp), E2 (CATGTG, −633 bp), or E3 (CACTTG, +249 bp) individually in the *Vegfc* promoter region and subcloned into the pGL3-Basic reporter plasmid. CMT93 cells were then cotransfected in duplicate with indicated Vegfc reporter plasmid and Hes1 expression plasmid (100 ng) or a control vector by using Lipofectamine LTX with PLUS Reagent (Thermo Fisher). 24 h after transfection, cell lysates were prepared and analyzed by using Dual-Luciferase Report Assay System. The Renilla luciferase reporter gene (pRL-TK; Promega) was used as an internal control.

Retroviral transduction

pMx-puroR retroviral vectors expressing full-length Hes1 cDNA, a dominant–negative Hes1 (dnHes1), and Hes1 deleted with the HLH domain or WRPW motif were generated as previously described (Shang et al., 2016a). Briefly, dnHes1 was generated by mutating E43, K44 and R47 in the basic region to A. Hes1(ΔHLH) and Hes1(ΔWPRW) deletion mutants were generated by deleting the HLH domain (amino acids 48–92) or the last six amino acids of Hes1, respectively. Vector expressing murine Vegfc was

generated by cloning Vegfc cDNA into pMx-puroR retroviral vector. For retroviral transduction, 3 × 10^6 Plat-E cells were seeded into 100-cm plates and cultured for 24 h. Cells were then transfected with 17 µg retroviral vectors of pMx-puro-GFP, pMx-puro-Flag-Hes1, or pMx-puro-Flag-Hes1 mutants or pMx-Vegfc using Fugene HD transfection reagent (Promega). 48 h after transfection, viral supernatants were collected and filtered, and 5 ml of viral supernatant was used to transduce 5 × 10^6 BMDMs in the presence of 8 µg/ml polybrene (Sigma-Aldrich). 24 h after viral infection, BMDMs were selected by puromycin (2 µg/ml) for 3 d and were then used for experiments.

Coimmunoprecipitation and immunoblotting analysis

HEK293T cells were transfected with pMx-puro-GFP, pMx-puro-Flag-Hes1, or pMx-puro-Flag-Hes1 mutants by using Fugene HD transfection reagent. 24 h after transfection, cells were harvested and then lysed in a lysis buffer containing 10 mM Tris, 150 mM NaCl, 1% NP-40, 5 mM EDTA, 1 mM PMSF, 1 mM $NaVO_3$, and the proteinase inhibitor cocktail (Roche). Extracts were immunoprecipitated with an anti-FLAG monoclonal antibody (F1804; Sigma-Aldrich) and protein A/G PLUS-Agarose beads (sc-2003; Santa Cruz Biotechnology). Whole-cell lysates or immunoprecipitated extracts were then separated by 10% SDS-PAGE and transferred to a polyvinylidene fluoride membrane (Millipore) for immunoblotting with specific antibodies. The antibodies used and the sources are as follows: Antibodies against p38 (1:1,000, sc-535), Hes1 (1:1,000, sc-25392), TLE (1:500, sc-13373), STAT1 (1:1,000, sc-346), TRAF3 (1:1,000, sc-6933), and IRF3 (1:1,000, sc-9082) were purchased from Santa Cruz Biotechnology. Antibodies against STAT2 (1:1,000, 72604), p-STAT1 (1:1,000, 7649), p-ERK (1:1,000, 9101), ERK (1:1,000, 9102), p-p38 (1:1,000, 9215), p-p65 (1:1,000, 3033), p65(1:1,000, 4764), IκBα (1:1,000, 4812), TBK1 (1:1,000, 3013), p-JNK (1:1,000, 9251), p-TBK1 (1:1,000, 5483), p-IKKε (1:1,000, 8766), IKKε (1:1,000, 3416), and p-IRF3 (1:500, 4947) were purchased from Cell Signaling Technology. Wdfy1 antibody (1:500, ab154716) was from Abcam, p-STAT2 antibody (1:1,000, 07–224) was from Millipore, TRIF antibody (1:1,000, NB120-13810) was from Novus, and anti-Tubulin antibody (1:2,000, be0025) was obtained from Easybio.

RNA-mediated interference

siRNA specifically targeting mouse Wdfy1 (69368) and nontargeting control siRNA were purchased from Dharmacon. siRNA oligoes were transfected into BMDMs using TransIT TKO transfection reagent according to the manufacturer's instructions (Mirus Bio). Cells were used 72 h after transfection.

ChIP-seq assay

The Hes1 ChIP-seq assay was performed and described in a previous study (Shang et al., 2016a). Hes1 ChIP-seq data were downloaded from the Gene Expression Omnibus (accession number GSE77334) and visualized by IGV (v2.3.78). The UCSC refseq annotated gene feature in *Mus musculus* mm10 was used to identify Hes1-binding peaks. For motif overrepresentation analysis, Hes1 binding with known motif enrichment was analyzed by Homer de novo Motif Enrichment Results.

Statistical analysis

P values were calculated with a two-tailed paired or unpaired Student's *t* test by Prism GraphPad software (v5.0). P values of ≤0.05 were considered significant. For the mouse survival study, Kaplan–Meier survival curves were generated by Prism 5.0 and analyzed for statistical significance with the log-rank test.

Online supplemental material

Fig. S1 shows that Hes1 suppresses TLR-induced IFN expression. Fig. S2 shows the IFN signature in vivo induced by TMPD administration. Fig. S3 shows that Hes1 does not directly regulate type I IFN and ISGs. Fig. S4 shows that Wdfy1 promotes the TMPD-induced IFN signature and protects against EMCV infection. Fig. S5 shows a summary of the present study for inhibition of type I IFN expression by Hes1. Table S1 lists the PCR primer sequences used in this study.

Acknowledgments

We thank R. Kageyama (Kyoto University, Kyoto, Japan) for *Hes1*$^{flox/flox}$ mice, H. Yang (China Agricultural University, Beijing, China) for the EMCV strain, and H. Wang (Shanghai Institutes for Biological Sciences, Chinese Academy of Sciences) for helpful discussion.

This research was supported by the Ministry of Science and Technology of China National Key Research Project (2015CB943201 to X. Hu), the National Natural Science Foundation of China (grants 31725010, 81422019, 81571580, 81661130161, and 91642115 to X. Hu), the Shandong Provincial Natural Science Foundation (grant ZR2017MC021 to Y. Shang), funds from the Tsinghua-Peking Center for Life Sciences (X. Hu), and funds from the Shandong "Double Tops" Program (Y. Shang).

The authors declare no competing financial interests.

Author contributions: F. Ning designed research, performed experiments, analyzed data, and wrote the manuscript; X. Li performed retrovirus infection experiments. L. Yu performed Hes1 ChIP-seq experiments. B. Zhang contributed to bioinformatics analysis. Y. Zhao constructed *Vegfc* promoter E box mutant plasmids. Y. Liu provided Wdfy1 overexpression plasmids and advice on experiments. B. Zhao provided advice on experiments and wrote the manuscript. Y. Shang initiated the project, performed experiments, analyzed data, supervised experiments, and wrote the manuscript. X. Hu conceptualized the project, designed research, supervised experiments, and wrote the manuscript.

Submitted: 9 May 2018
Revised: 22 October 2018
Accepted: 4 April 2019

References

Alvarez, Y., C. Municio, E. Hugo, J. Zhu, S. Alonso, X. Hu, N. Fernández, and M. Sánchez Crespo. 2011. Notch- and transducin-like enhancer of split (TLE)-dependent histone deacetylation explain interleukin 12 (IL-12) p70 inhibition by zymosan. *J. Biol. Chem.* 286:16583–16595. https://doi.org/10.1074/jbc.M111.222158

Arisi, I., M. D'Onofrio, R. Brandi, A. Felsani, S. Capsoni, G. Drovandi, G. Felici, E. Weitschek, P. Bertolazzi, and A. Cattaneo. 2011. Gene expression biomarkers in the brain of a mouse model for Alzheimer's

disease: mining of microarray data by logic classification and feature selection. *J. Alzheimers Dis.* 24:721–738. https://doi.org/10.3233/JAD-2011-101881

Bennett, J.A., K.P. Singh, Z. Unnisa, S.L. Welle, and T.A. Gasiewicz. 2015. Deficiency in Aryl Hydrocarbon Receptor (AHR) Expression throughout Aging Alters Gene Expression Profiles in Murine Long-Term Hematopoietic Stem Cells. *PLoS One.* 10:e0133791. https://doi.org/10.1371/journal.pone.0133791

Boxx, G.M., and G. Cheng. 2016. The Roles of Type I Interferon in Bacterial Infection. *Cell Host Microbe.* 19:760–769. https://doi.org/10.1016/j.chom.2016.05.016

Buscarlet, M., and S. Stifani. 2007. The 'Marx' of Groucho on development and disease. *Trends Cell Biol.* 17:353–361. https://doi.org/10.1016/j.tcb.2007.07.002

Chen, K., J. Liu, and X. Cao. 2017. Regulation of type I interferon signaling in immunity and inflammation: A comprehensive review. *J. Autoimmun.* 83:1–11. https://doi.org/10.1016/j.jaut.2017.03.008

Crow, M.K. 2014. Type I interferon in the pathogenesis of lupus. *J. Immunol.* 192:5459–5468. https://doi.org/10.4049/jimmunol.1002795

Davidson, A. 2016. What is damaging the kidney in lupus nephritis? *Nat. Rev. Rheumatol.* 12:143–153. https://doi.org/10.1038/nrrheum.2015.159

Dutta, S., S. Roy, N.S. Polavaram, G.B. Baretton, M.H. Muders, S. Batra, and K. Datta. 2016. NRP2 transcriptionally regulates its downstream effector WDFY1. *Sci. Rep.* 6:23588. https://doi.org/10.1038/srep23588

Fisher, A.L., S. Ohsako, and M. Caudy. 1996. The WRPW motif of the hairy-related basic helix-loop-helix repressor proteins acts as a 4-amino-acid transcription repression and protein-protein interaction domain. *Mol. Cell. Biol.* 16:2670–2677. https://doi.org/10.1128/MCB.16.6.2670

Furie, R., M. Khamashta, J.T. Merrill, V.P. Werth, K. Kalunian, P. Brohawn, G.G. Illei, J. Drappa, L. Wang, and S. Yoo. CD1013 Study Investigators. 2017. Anifrolumab, an Anti-Interferon-α Receptor Monoclonal Antibody, in Moderate-to-Severe Systemic Lupus Erythematosus. *Arthritis Rheumatol.* 69:376–386. https://doi.org/10.1002/art.39962

Gough, D.J., N.L. Messina, C.J. Clarke, R.W. Johnstone, and D.E. Levy. 2012. Constitutive type I interferon modulates homeostatic balance through tonic signaling. *Immunity.* 36:166–174. https://doi.org/10.1016/j.immuni.2012.01.011

Guo, X.K., J. Ou, S. Liang, X. Zhou, and X. Hu. 2018. Epithelial Hes1 maintains gut homeostasis by preventing microbial dysbiosis. *Mucosal Immunol.* 11:716–726. https://doi.org/10.1038/mi.2017.111

Hall, J.C., and A. Rosen. 2010. Type I interferons: crucial participants in disease amplification in autoimmunity. *Nat. Rev. Rheumatol.* 6:40–49. https://doi.org/10.1038/nrrheum.2009.237

Hardarson, H.S., J.S. Baker, Z. Yang, E. Purevjav, C.H. Huang, L. Alexopoulou, N. Li, R.A. Flavell, N.E. Bowles, and J.G. Vallejo. 2007. Toll-like receptor 3 is an essential component of the innate stress response in virus-induced cardiac injury. *Am. J. Physiol. Heart Circ. Physiol.* 292:H251–H258. https://doi.org/10.1152/ajpheart.00398.2006

Honda, K., A. Takaoka, and T. Taniguchi. 2006. Type I interferon [corrected] gene induction by the interferon regulatory factor family of transcription factors. *Immunity.* 25:349–360. https://doi.org/10.1016/j.immuni.2006.08.009

Hu, X., A.Y. Chung, I. Wu, J. Foldi, J. Chen, J.D. Ji, T. Tateya, Y.J. Kang, J. Han, M. Gessler, et al 2008. Integrated regulation of Toll-like receptor responses by Notch and interferon-gamma pathways. *Immunity.* 29:691–703. https://doi.org/10.1016/j.immuni.2008.08.016

Hu, Y.H., Y. Zhang, L.Q. Jiang, S. Wang, C.Q. Lei, M.S. Sun, H.B. Shu, and Y. Liu. 2015. WDFY1 mediates TLR3/4 signaling by recruiting TRIF. *EMBO Rep.* 16:447–455. https://doi.org/10.15252/embr.201439637

Ikushima, H., H. Negishi, and T. Taniguchi. 2013. The IRF family transcription factors at the interface of innate and adaptive immune responses. *Cold Spring Harb. Symp. Quant. Biol.* 78:105–116. https://doi.org/10.1101/sqb.2013.78.020321

Indra, A.K., X. Warot, J. Brocard, J.M. Bornert, J.H. Xiao, P. Chambon, and D. Metzger. 1999. Temporally-controlled site-specific mutagenesis in the basal layer of the epidermis: comparison of the recombinase activity of the tamoxifen-inducible Cre-ER(T) and Cre-ER(T2) recombinases. *Nucleic Acids Res.* 27:4324–4327. https://doi.org/10.1093/nar/27.22.4324

Ishibashi, M., S.L. Ang, K. Shiota, S. Nakanishi, R. Kageyama, and F. Guillemot. 1995. Targeted disruption of mammalian hairy and Enhancer of split homolog-1 (HES-1) leads to up-regulation of neural helix-loop-helix factors, premature neurogenesis, and severe neural tube defects. *Genes Dev.* 9:3136–3148. https://doi.org/10.1101/gad.9.24.3136

Ivashkiv, L.B., and L.T. Donlin. 2014. Regulation of type I interferon responses. *Nat. Rev. Immunol.* 14:36–49. https://doi.org/10.1038/nri3581

Jin, J., H. Hu, H.S. Li, J. Yu, Y. Xiao, G.C. Brittain, Q. Zou, X. Cheng, F.A. Mallette, S.S. Watowich, and S.C. Sun. 2014. Noncanonical NF-κB pathway controls the production of type I interferons in antiviral innate immunity. *Immunity.* 40:342–354. https://doi.org/10.1016/j.immuni.2014.02.006

Ju, B.G., D. Solum, E.J. Song, K.J. Lee, D.W. Rose, C.K. Glass, and M.G. Rosenfeld. 2004. Activating the PARP-1 sensor component of the groucho/TLE1 corepressor complex mediates a CaMKinase IIdelta-dependent neurogenic gene activation pathway. *Cell.* 119:815–829. https://doi.org/10.1016/j.cell.2004.11.017

Kalunian, K.C., J.T. Merrill, R. Maciuca, J.M. McBride, M.J. Townsend, X. Wei, J.C. Davis Jr., and W.P. Kennedy. 2016. A Phase II study of the efficacy and safety of rontalizumab (rhuMAb interferon-α) in patients with systemic lupus erythematosus (ROSE). *Ann. Rheum. Dis.* 75:196–202. https://doi.org/10.1136/annrheumdis-2014-206090

Kawai, T., and S. Akira. 2011. Toll-like receptors and their crosstalk with other innate receptors in infection and immunity. *Immunity.* 34:637–650. https://doi.org/10.1016/j.immuni.2011.05.006

Khamashta, M., J.T. Merrill, V.P. Werth, R. Furie, K. Kalunian, G.G. Illei, J. Drappa, L. Wang, and W. Greth. CD1067 study investigators. 2016. Sifalimumab, an anti-interferon-α monoclonal antibody, in moderate to severe systemic lupus erythematosus: a randomised, double-blind, placebo-controlled study. *Ann. Rheum. Dis.* 75:1909–1916. https://doi.org/10.1136/annrheumdis-2015-208562

Kobayashi, T., and R. Kageyama. 2014. Expression dynamics and functions of Hes factors in development and diseases. *Curr. Top. Dev. Biol.* 110:263–283. https://doi.org/10.1016/B978-0-12-405943-6.00007-5

Kondo, T., T. Kawai, and S. Akira. 2012. Dissecting negative regulation of Toll-like receptor signaling. *Trends Immunol.* 33:449–458. https://doi.org/10.1016/j.it.2012.05.002

McNab, F., K. Mayer-Barber, A. Sher, A. Wack, and A. O'Garra. 2015. Type I interferons in infectious disease. *Nat. Rev. Immunol.* 15:87–103. https://doi.org/10.1038/nri3787

Nacionales, D.C., K.M. Kelly-Scumpia, P.Y. Lee, J.S. Weinstein, R. Lyons, E. Sobel, M. Satoh, and W.H. Reeves. 2007. Deficiency of the type I interferon receptor protects mice from experimental lupus. *Arthritis Rheum.* 56:3770–3783. https://doi.org/10.1002/art.23023

Nandakumar, R., and S.R. Paludan. 2015. Catching the adaptor-WDFY1, a new player in the TLR-TRIF pathway. *EMBO Rep.* 16:397–398. https://doi.org/10.15252/embr.201540145

Petri, M., D.J. Wallace, A. Spindler, V. Chindalore, K. Kalunian, E. Mysler, C.M. Neuwelt, G. Robbie, W.I. White, B.W. Higgs, et al 2013. Sifalimumab, a human anti-interferon-α monoclonal antibody, in systemic lupus erythematosus: a phase I randomized, controlled, dose-escalation study. *Arthritis Rheum.* 65:1011–1021. https://doi.org/10.1002/art.37824

Porritt, R.A., and P.J. Hertzog. 2015. Dynamic control of type I IFN signalling by an integrated network of negative regulators. *Trends Immunol.* 36:150–160. https://doi.org/10.1016/j.it.2015.02.002

Ramasamy, S., B. Saez, S. Mukhopadhyay, D. Ding, A.M. Ahmed, X. Chen, F. Pucci, R. Yamin, J. Wang, M.J. Pittet, et al 2016. Tle1 tumor suppressor negatively regulates inflammation in vivo and modulates NF-κB inflammatory pathway. *Proc. Natl. Acad. Sci. USA.* 113:1871–1876. https://doi.org/10.1073/pnas.1511380113

Reeves, W.H., P.Y. Lee, J.S. Weinstein, M. Satoh, and L. Lu. 2009. Induction of autoimmunity by pristane and other naturally occurring hydrocarbons. *Trends Immunol.* 30:455–464. https://doi.org/10.1016/j.it.2009.06.003

Ridley, S.H., N. Ktistakis, K. Davidson, K.E. Anderson, M. Manifava, C.D. Ellson, P. Lipp, M. Bootman, J. Coadwell, A. Nazarian, et al 2001. FENS-1 and DFCP1 are FYVE domain-containing proteins with distinct functions in the endosomal and Golgi compartments. *J. Cell Sci.* 114:3991–4000.

Rönnblom, L., G.V. Alm, and M.L. Eloranta. 2011. The type I interferon system in the development of lupus. *Semin. Immunol.* 23:113–121. https://doi.org/10.1016/j.smim.2011.01.009

Rusinova, I., S. Forster, S. Yu, A. Kannan, M. Masse, H. Cumming, R. Chapman, and P.J. Hertzog. 2013. Interferome v2.0: an updated database of annotated interferon-regulated genes. *Nucleic Acids Res.* 41(D1):D1040–D1046. https://doi.org/10.1093/nar/gks1215

Schellenburg, S., A. Schulz, D.M. Poitz, and M.H. Muders. 2017. Role of neuropilin-2 in the immune system. *Mol. Immunol.* 90:239–244. https://doi.org/10.1016/j.molimm.2017.08.010

Schneider, W.M., M.D. Chevillotte, and C.M. Rice. 2014. Interferon-stimulated genes: a complex web of host defenses. *Annu. Rev. Immunol.* 32:513–545. https://doi.org/10.1146/annurev-immunol-032713-120231

Seth, R.B., L. Sun, C.K. Ea, and Z.J. Chen. 2005. Identification and characterization of MAVS, a mitochondrial antiviral signaling protein that

activates NF-kappaB and IRF 3. *Cell.* 122:669–682. https://doi.org/10.1016/j.cell.2005.08.012

Shang, Y., M. Coppo, T. He, F. Ning, L. Yu, L. Kang, B. Zhang, C. Ju, Y. Qiao, B. Zhao, et al 2016a. The transcriptional repressor Hes1 attenuates inflammation by regulating transcription elongation. *Nat. Immunol.* 17: 930–937. https://doi.org/10.1038/ni.3486

Shang, Y., S. Smith, and X. Hu. 2016b. Role of Notch signaling in regulating innate immunity and inflammation in health and disease. *Protein Cell.* 7: 159–174. https://doi.org/10.1007/s13238-016-0250-0

Sodsai, P., N. Hirankarn, Y. Avihingsanon, and T. Palaga. 2008. Defects in Notch1 upregulation upon activation of T Cells from patients with systemic lupus erythematosus are related to lupus disease activity. *Lupus.* 17:645–653. https://doi.org/10.1177/0961203308089406

Sprangers, B., M. Monahan, and G.B. Appel. 2012. Diagnosis and treatment of lupus nephritis flares--an update. *Nat. Rev. Nephrol.* 8:709–717. https://doi.org/10.1038/nrneph.2012.220

Stanton, M.J., S. Dutta, H. Zhang, N.S. Polavaram, A.A. Leontovich, P. Hönscheid, F.A. Sinicrope, D.J. Tindall, M.H. Muders, and K. Datta. 2013. Autophagy control by the VEGF-C/NRP-2 axis in cancer and its implication for treatment resistance. *Cancer Res.* 73:160–171. https://doi.org/10.1158/0008-5472.CAN-11-3635

Urbonaviciute, V., C. Starke, W. Pirschel, S. Pohle, S. Frey, C. Daniel, K. Amann, G. Schett, M. Herrmann, and R.E. Voll. 2013. Toll-like receptor 2 is required for autoantibody production and development of renal disease in pristane-induced lupus. *Arthritis Rheum.* 65:1612–1623. https://doi.org/10.1002/art.37914

Wong, M.T., and S.S. Chen. 2016. Emerging roles of interferon-stimulated genes in the innate immune response to hepatitis C virus infection. *Cell. Mol. Immunol.* 13:11–35. https://doi.org/10.1038/cmi.2014.127

Yao, X., and S. Bouyain. 2015. Splicing and proteolytic processing in VEGF signaling: now it is the coreceptor's turn. *Structure.* 23:610–611. https://doi.org/10.1016/j.str.2015.03.003

Zhang, X., X. Li, F. Ning, Y. Shang, and X. Hu. 2019. TLE4 acts as a co-repressor of Hes1 to inhibit inflammatory responses in macrophages. *Protein Cell.* 10:300–305. https://doi.org/10.1007/s13238-018-0554-3

Zhang, Y., Y. Lu, L. Ma, X. Cao, J. Xiao, J. Chen, S. Jiao, Y. Gao, C. Liu, Z. Duan, et al 2014. Activation of vascular endothelial growth factor receptor-3 in macrophages restrains TLR4-NF-κB signaling and protects against endotoxin shock. *Immunity.* 40:501–514. https://doi.org/10.1016/j.immuni.2014.01.013